EPR Spectroscopy Hot Paper

DOI: 10.1002/anie.201305574

Gadolinium(III) Spin Labels for High-Sensitivity Distance Measurements in Transmembrane Helices**

*Erez Matalon, Thomas Huber, Gregor Hagelueken, Bim Graham, Veronica Frydman, Akiva Feintuch, Gottfried Otting, and Daniella Goldfarb**

Distance determination, by pulse EPR techniques, between two spin labels attached to biomolecules has become an attractive methodology to probe conformations and assemblies of biomolecules in frozen solutions.[1–3] Among these techniques, double electron-electron resonance (DEER or PELDOR),[4,5] which can access distances in the range of 1.7 to 8 nm, is highly popular,[6–8] and the most widely used spin labels are nitroxide radicals. Membrane proteins in their natural environment are of particular interest for DEER applications, since those pose a considerable challenge for X-ray crystallography and NMR spectroscopy. DEER studies of peptides and proteins in either reconstituted or model membranes[9–11] are considerably more challenging than those in solution, because the high local concentration of the spins in the membrane decreases the phase memory time and, therefore, sensitivity.[12] Most DEER measurements on nitroxide-labeled biomolecules are carried out at X-band frequencies (9.5 GHz, 0.35 T), and recently such measurements were demonstrated in frozen cells.[13,14] A major difficulty of such measurements is the reduction of nitroxides in the cell, which severely limits the scope of such exciting developments.

Recently, Gd^{3+} ($S = 7/2$) spin labels have been suggested as an alternative to nitroxide spin labels for W-band and Q-band DEER distance measurements.[15–19] Gd^{3+} tags can be attached to proteins, similar to nitroxides, by site-directed spin labeling (SDSL).[20] Gd^{3+} features high sensitivity at high frequencies and the DEER measurements are free of orientation selection effects so that the distance distribution can readily be extracted from a single DEER measurement. Moreover, in the context of future development of in-cell DEER measurements, Gd^{3+} chelates are stable under in vivo conditions as known from their applications as contrast agents for magnetic resonance imaging (MRI). Gd^{3+}-Gd^{3+} DEER has been demonstrated on model systems, proteins, peptides, and DNA, all in isotropic membrane-free solutions.[15–19] Distance measurements between a Gd^{3+} label and a nitroxide label have also been shown to yield attractive sensitivity.[21–23]

In this work, we continue to develop the approach of Gd^{3+}–Gd^{3+} DEER distance measurements and demonstrate for the first time such measurements in a model membrane. The model system we chose consists of the well-studied transmembrane helical WALP peptides in 1,2-dioleoyl-*sn*-glycero-3-phosphocholine (DOPC) vesicles.[24,25] We demonstrate the sensitivity of W-band Gd^{3+}–Gd^{3+} DEER to small distance variations in a membrane. Using WALP peptides of different lengths we show that such measurements pick up, in addition to the helix extension, also subtle "*cis–trans*" effects arising from different positions of the labels with respect to the helix axes. In addition, we report the effect of the spin label interaction with the membranes on the measured distance distribution. We compared W-band DEER on WALP23 labeled with two different Gd^{3+} tags with X-band DEER on WALP23 labeled with nitroxide tags. Here we used X-band, rather than W-band, to avoid complications owing to orientation selection.[16] The differences observed are important and suggest that by employing different spin labels such effects can be isolated. Finally, we show that the effect of hydrophobic mismatch[26] between peptide and membrane can be explored by Gd^{3+}–Gd^{3+} DEER.

WALP23 was labeled at the N and C termini (see Table 1) with two nitroxides (WAL23-NO) using (l-oxyl-2,2,5,5-tetramethyl-3-pyrroline-3-methyl)methanesulfonate (MTSSL) and two different Gd-DOTA derivatives, shown in Figure 1. WALP23-DOTA is labeled with a DOTA chelate and WALP23-C1 with DOTA with phenylethylamine substituents. The bulky substituents were designed to restrict the flexibility of the tag.[27] The hydrophobic length of WALP23 (ca. 2.6 nm) is very close to that of the hydrophobic thickness of DOPC bilayers (ca. 2.7 nm).[25,26,28] The sample composition was 50 μM WALP23 in DOPC multilamellar vesicles (MLV; 1:1000 peptide/lipid molar ratio). Details of the sample preparation are given in the Supporting Information.

[*] Dr. E. Matalon, Dr. A. Feintuch, Prof. D. Goldfarb
Department of Chemical Physics, Weizmann Institute of Science
Rehovot, 76100 (Israel)
E-mail: Daniella.goldfarb@weizmann.ac.il
Dr. V. Frydman
Department of Chemical Research Support
Weizmann Institute of Science (Israel)
Dr. T. Huber, Prof. G. Otting
Research School of Chemistry, The Australian National University
Canberra ACT 0200 (Australia)
Dr. B. Graham
Monash Institute of Pharmaceutical Sciences
Monash University
Parkville 3052 VIC (Australia)
Dr. G. Hagelueken
Institute of Physical and Theoretical Chemistry, University of Bonn
Wegerlerstr. 12, 53112 Bonn (Germany)

[**] This work was supported by the Israel Science Foundation (ISF). D.G. holds the Erich Klieger Professorial Chair in Chemical Physics. This research was made possible in part by the historic generosity of the Harold Perlman Family. We thank Dr. M. Eisenstein for her help with the WALP modeling. Financial support by the Australian Research Council, including a Future Fellowship to T.H. is gratefully acknowledged.

Supporting information for this article is available on the WWW under http://dx.doi.org/10.1002/anie.201305574.

Table 1: Sequences of WALP peptides.

Peptide	Sequence[a]	Length of central stretch [nm][b]
WALP19-C1(DOTA)	Ac-C(sl)WWLALALALALALWWC(sl)-NH_2	19.5
WALP21-C1(DOTA)	Ac-C(sl)WWLALALALALALALWWC(sl)-NH_2	22.5
WALP23-C1(DOTA)	Ac-C(sl)WWLALALALALALALALWWC(sl)-NH_2	25.5
WALP25-C1(DOTA)	Ac-C(sl)WWLALALALALALALALALWWC(sl)-NH_2	28.5
WALP27-C1[c]	Ac-C(sl)WWLALALALALALALALALALWWC(sl)-NH_2	31.5

[a] C(sl) is the spin-labeled cysteine residue. [b] An ideal α helix is assumed, where each amino acid contributes 1.5 Å to the pitch of the helix. The central stretch is defined by the Leu and Ala residues. [c] The WALP27-DOTA construct did not insert into the MLVs sufficiently well.

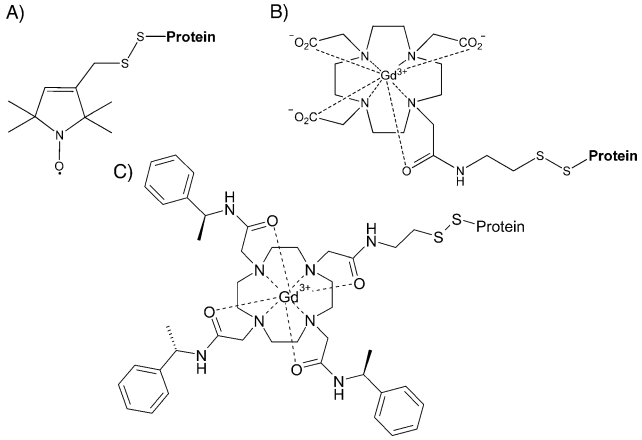

Figure 1. Spin labels used in this study. A) MTSSL. B) DOTA tag loaded with Gd^{3+}. C) C1 tag loaded with Gd^{3+}.

The X-band DEER trace of WALP23-NO, and the W-band DEER traces of WALP23-C1 and WALP23-DOTA are shown in Figure 2 A,B (see Figure S1 in the Supporting Information for further details and raw data). Although the modulation depth of the Gd^{3+}-labeled samples, approximately 4 %, is considerably smaller than that of WALP23-NO (ca. 20 %), their overall signal-to-noise ratio (SNR) per peptide amount and accumulation time is much higher (see the Supporting Information for details). This is because of their large echo intensity, shorter repetition delay, and the longer echo decay (Figure S2 and Table S1 in the Supporting Information). Figure 2 C shows that the distance distribution of WALP23-NO exhibits a maximum at 3.1 nm, whereas for WALP23-C1 and WALP23-DOTA it is at 3.7 nm and 4.3 nm, respectively. To ensure that these are intramolecular distances and that aggregates were absent, we carried out a control DEER measurement on WALP23-C1 singly labeled at position 23 (Figure S3 in the Supporting Information).

The variation in the distances measured between the different labels (Figure 2 C,D) can be attributed to their different interactions with the membrane, rather than their slightly different tether lengths. To substantiate this and to account for the broad distance distributions, we modeled WALP23 as a perfect α helix to which the three different pairs of labels were attached and allowed all sterically possible label rotamers. We applied two modeling approaches: The first, termed "mW model", used mtsslWizard, which is a PyMOL plug-in[29] and was extended to include the DOTA label. It identifies all possible rotamers of the label that do not clash with the peptide (within a given tolerance) and does not make assumptions about rotamer probabilities or interaction energies. This approach was used for calculating the distance distribution of WALP23-NO and WALP23-DOTA (Figure S5 in the Supporting Information). The second approach, termed "PyPara model", used PyParaTools [http://comp-bio.anu.edu.au/mscook/PPT] and was applied to WALP23-C1 and WALP23-NO. This approach, in addition to producing tag conformers free of steric clashes with the protein, accounts more accurately for local torsion angle preferences in the attached labels (more details are given in the Supporting Information).

Figure 2 C compares the calculated and experimental distance distributions of the three peptides. The two models predict very similar distance distributions for WALP23-NO where the maximum of the distance distribution is shifted towards slightly shorter distances than the other two because of the shorter tether of the MTSSL tag (Figure 1). In contrast, the experimental results are more dispersed, with a particularly large discrepancy between modeled and experimental distances for WALP23-NO. This can be explained by the more hydrophobic nature of the nitroxide tag, which is expected to interact favorably with the membrane generating

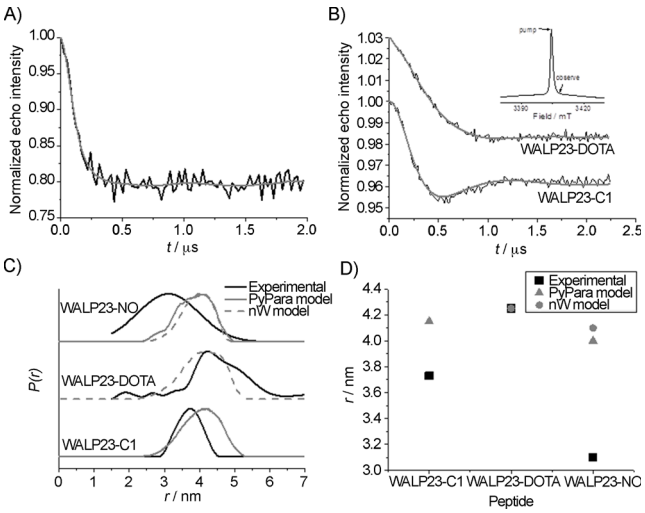

Figure 2. DEER results obtained for WALP23 in DOPC. Background-corrected normalized A) X-band DEER trace for WALP23-NO and B) W-band DEER traces for WALP23-C1 and WALP23-DOTA tags. The inset in (B) shows the echo detected EPR spectrum and the positions of the pump and observe pulses. For improved visualization, the trace of the WALP23-DOTA experiment was shifted up by 0.03 units. Gray lines represent the fit with the distance distributions shown in (C) in black. Gray lines in (C) show the modeled distance distributions (PyPara model: gray solid line; mW model: gray dashed line). D) Summary of distances with maximum probability obtained from the fitted (black ■) and modeled results (PyPara model: gray ▲; mW model: gray ●).

a so-called conformational bias. Similarly, the C1 tag is more hydrophobic than the DOTA tag, thus explaining the observed shift towards shorter distances. The positive charge of the C1 tag may enhance this effect by interactions with the phosphodiester groups of the DOPC bilayers, which are more buried than the positively charged choline groups.

A hydrophobic bias of the MTSSL label was previously suggested for spin-labeled melittin in vesicles.[30,31] The reported positional shift of 0.5–0.6 nm by a nitroxide radical is consistent with the shortening of the nitroxide–nitroxide distance by 1–1.2 nm observed in our experiments. The WALP23-DOTA sample produced the best match between calculated and experimentally derived distance distribution maxima, although the experimental distance distribution is broad, with a shoulder towards longer distances. In contrast to the C1 tag, the DOTA tag can assume different chiralities of similar energy, leading to diastereomers with the peptide that can favor different distance distributions. This tag, which is more hydrophilic than the nitroxide and C1 tags, seems to be accommodated in the region of the lipid head groups without particular preference for either the lipid phase or the aqueous phase of the bulk water. The DOTA and C1 tags produced smaller differences between experimental results in a membrane and predicted distances in the absence of a membrane than the nitroxide tag.

To explore the sensitivity of Gd^{3+}–Gd^{3+} distance measurements to variations in helix length we prepared a series of WALP peptides of different lengths labeled at both ends with either C1 or DOTA tags (Table 1). WALP19 and WALP21 should exhibit a negative mismatch,[28] where the hydrophobic thickness of the membrane is larger than that of the transmembrane helix, whereas for WALP25 and WALP27 a positive mismatch is expected.[28] Figure 3 A,C show the DEER traces for each of these peptides (the raw data are shown in Figure S4 and the two-pulse echo decays are presented in Figure S2 in the Supporting Information). The corresponding experimental and modeled distance distributions are shown in Figure 3 B,D.

The experimentally determined distance distributions of the WALP-C1 peptides are consistently shifted towards shorter distances than the modeled distance distributions, with increasing discrepancies for the longer WALP peptides (Figure 4 A). As discussed earlier this is due to favorable interactions of the tag with the membrane because of the fairly hydrophobic substituents of the tag and its positive charge. Therefore, maintaining the contact between tag and membrane for the longer helices requires an increasing conformational bias of the tag. In contrast, the WALP-DOTA samples tended to show longer experimental distances than expected from modeling, thus indicating an overall preference of the DOTA tag for the aqueous phase (Figure 4 B). Remarkably, and irrespective of the mismatches, the experimental data obtained with either tags show clear evidence for nonlinear distance variations expected for helical peptides. This arises from tag molecules located on either the same (*cis*) or opposite (*trans*) sides of the α helix (Figure S6 in the Supporting Information). For example, the two spin labels are on the same side of the helix for WALP19-C1, whereas they are on opposite sides in WALP21-C1, which

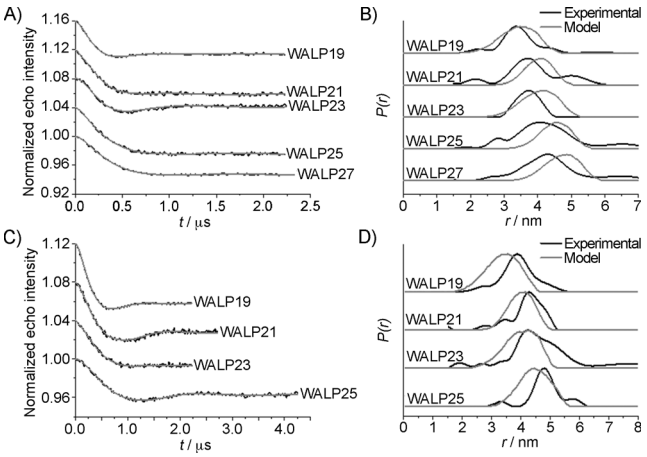

Figure 3. W-band DEER results obtained for WALP-C1 and WALP-DOTA in DOPC membranes. A) Background-corrected, normalized DEER traces obtained for the WALP-C1 series. The experimental conditions were the same as in Figure 2. For improved visualization, the traces were shifted by 0.04 units from each other. The gray lines represent the fits with the distance distributions shown in (B) in black. B) Experimental (black) and PyPara model (gray) distance distributions of the WALP-C1 series. C) and D) same as (A) and (B), respectively, except for the WALP-DOTA series and the model is the mW model.

is two amino acids longer. This is also illustrated in the helical-wheel projection of the peptide (Figure S7 in the Supporting Information). The effect decreases with increasing helix length (Figure 4 C).

The *cis–trans* effect is equally apparent for the WALP-DOTA series, with a remarkably constant difference of 0.5–0.6 nm compared to WALP-C1 maintained throughout the series (Figure 4 D). This effect is somewhat less pronounced

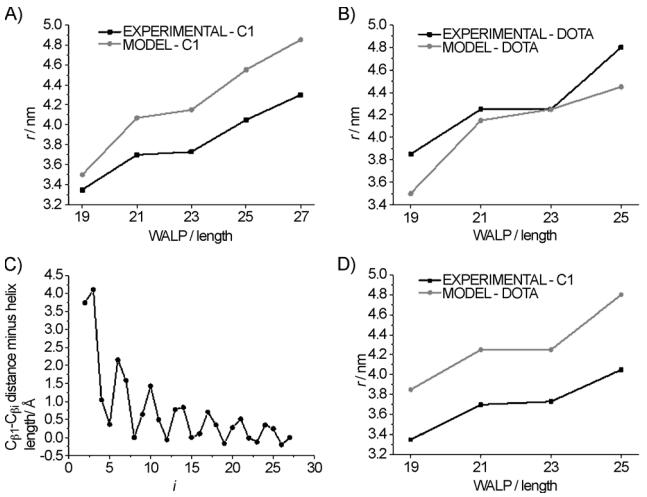

Figure 4. Gd^{3+}–Gd^{3+} distance measurements reflect α helix periodicity. A) Summary of experimental (black) and modeling (gray) results for the WALP peptides with C1 tag. B) Same as (A), but for the DOTA tag. C) Modeled distance variations (maxima of distance distributions) in WALP27. The vertical axis represents the $C_{\beta1}$–$C_{\beta i}$ distance minus the length of the helix up to position *i*, where *i* is the residue number. It is approximated by the $C_{\beta1}$–$C_{\beta27}$ distance * i/27. D) Comparison of experimental distances for WALP-C1 (black) and WALP-DOTA (gray) as a function of WALP length.

in the modeled data of WALP-DOTA (Figure S8 in the Supporting Information). The clarity of the *cis–trans* effect indicates α-helical secondary structure of the peptides even for those WALP peptides that span a longer distance than the thickness of the membrane (WALP25 and WALP27). One of the responses to such a positive mismatch is tilting of the helix in the membrane.[28] We conclude that the helices tilt rather than bend and that the offset between the different tags is caused by conformational bias of the tags introduced by their different affinity for the membrane. Recent X- and Q-band Gd^{3+} nitroxide DEER measurements on a series of WALP23 peptides, which were labeled with a Gd^{3+} tag at one end and a nitroxide at different positions along the peptide, in DOPC vesicles reported the pitch of the helix, thus confirming the helical structure of the peptide.[22]

In summary, this study demonstrates the potential of W-band Gd^{3+}–Gd^{3+} DEER distance measurements in a membrane environment. Such measurements feature high absolute sensitivity and should be feasible for tracking conformational changes in membrane proteins, using minute amounts of labeled protein (> 0.15 nmol) and acceptable measurement times. Gd^{3+} tags also offer the chemical flexibility to choose the appropriate tag for particular applications.

Received: June 28, 2013
Revised: August 14, 2013
Published online: September 17, 2013

Keywords: DEER · EPR spectroscopy · gadolinium · membrane proteins · spin labeling

[1] P. P. Borbat, J. H. Freed, *Methods Enzymol.* **2007**, *423*, 52 – 116.
[2] P. P. Borbat, H. S. Mchaourab, J. H. Freed, *J. Am. Chem. Soc.* **2002**, *124*, 5304 – 5314.
[3] G. Jeschke, *Annu. Rev. Phys. Chem.* **2012**, *63*, 419 – 446.
[4] A. D. Milov, A. B. Ponomarev, Y. D. Tsvetkov, *Chem. Phys. Lett.* **1984**, *110*, 67 – 72.
[5] M. Pannier, S. Veit, A. Godt, G. Jeschke, H. W. Spiess, *J. Magn. Reson.* **2000**, *142*, 331 – 340.
[6] P. P. Borbat, E. R. Georgieva, J. H. Freed, *J. Phys. Chem. Lett.* **2013**, *4*, 170 – 175.
[7] A. Bowman, R. Ward, H. El-Mkami, T. Owen-Hughes, D. G. Norman, *Nucleic Acids Res.* **2010**, *38*, 695 – 707.
[8] W. Richard, A. Bowman, E. Sozudogru, H. El-Mkami, T. Owen-Hughes, D. G. Norman, *J. Magn. Reson.* **2010**, *207*, 164 – 167.
[9] E. R. Georgieva, T. F. Ramlall, P. P. Borbat, J. H. Freed, D. Eliezer, *J. Am. Chem. Soc.* **2008**, *130*, 12856 – 12857.
[10] M. Grote, Y. Polyhach, G. Jeschke, H. J. Steinhoff, E. Schneider, E. Bordignon, *J. Biol. Chem.* **2009**, *284*, 17521 – 17526.
[11] P. Zou, H. S. Mchaourab, *Biophys. J.* **2010**, *98*, L18 – L20.
[12] R. Dastvan, B. E. Bode, M. P. R. Karuppiah, A. Marko, S. Lyubenova, H. Schwalbe, T. F. Prisner, *J. Phys. Chem. B* **2010**, *114*, 13507 – 13516.
[13] R. Igarashi, T. Sakai, H. Hara, T. Tenno, T. Tanaka, H. Tochio, M. Shirakawa, *J. Am. Chem. Soc.* **2010**, *132*, 8228 – 8229.
[14] I. Krstić, R. Hänsel, O. Romainczyk, J. W. Engels, V. Dötsch, T. F. Prisner, *Angew. Chem.* **2011**, *123*, 5176 – 5180; *Angew. Chem. Int. Ed.* **2011**, *50*, 5070 – 5074.
[15] A. M. Raitsimring, C. Gunanathan, A. Potapov, I. Efremenko, J. M. Martin, D. Milstein, D. Goldfarb, *J. Am. Chem. Soc.* **2007**, *129*, 14138 – 14139.
[16] A. Potapov, H. Yagi, T. Huber, S. Jergic, N. E. Dixon, G. Otting, D. Goldfarb, *J. Am. Chem. Soc.* **2010**, *132*, 9040 – 9048.
[17] Y. Song, T. J. Meade, A. V. Astashkin, E. L. Klein, J. H. Enemark, A. Raitsimring, *J. Magn. Reson.* **2011**, *210*, 59 – 68.
[18] H. Yagi, D. Banerjee, B. Graham, T. Huber, D. Goldfarb, G. Otting, *J. Am. Chem. Soc.* **2011**, *133*, 10418 – 10421.
[19] M. Gordon-Grossman, I. Kaminker, Y. Gofman, Y. Shai, D. Goldfarb, *Phys. Chem. Chem. Phys.* **2011**, *13*, 10771 – 10780.
[20] G. Otting, *Annu. Rev. Biophys.* **2010**, *39*, 387 – 405.
[21] I. Kaminker, I. Tkach, N. Manukovsky, T. Huber, H. Yagi, G. Otting, M. Bennati, D. Goldfarb, *J. Magn. Reson.* **2013**, *227*, 66 – 71.
[22] P. Lueders, H. Jager, M. A. Hemminga, G. Jeschke, M. Yulikov, *J. Phys. Chem. B* **2013**, *117*, 2061 – 2068.
[23] P. Lueders, G. Jeschke, M. Yulikov, *J. Phys. Chem. Lett.* **2011**, *2*, 604 – 609.
[24] M. R. R. de Planque, E. Goormaghtigh, D. V. Greathouse, R. E. Koeppe, J. A. W. Kruijtzer, R. M. J. Liskamp, B. de Kruijff, J. A. Killian, *Biochemistry* **2001**, *40*, 5000 – 5010.
[25] R. D. Nielsen, K. P. Che, M. H. Gelb, B. H. Robinson, *J. Am. Chem. Soc.* **2005**, *127*, 6430 – 6442.
[26] O. G. Mouritsen, M. Bloom, *Biophys. J.* **1984**, *46*, 141 – 153.
[27] B. Graham, C. T. Loh, J. D. Swarbrick, P. Ung, J. Shin, H. Yagi, X. Jia, S. Chhabra, N. Barlow, G. Pintacuda, T. Huber, G. Otting, *Bioconjugate Chem.* **2011**, *22*, 2118 – 2125.
[28] M. R. R. de Planque, J. A. Killian, *Mol. Membr. Biol.* **2003**, *20*, 271 – 284.
[29] G. Hagelueken, R. Ward, J. H. Naismith, O. Schiemann, *Appl. Magn. Reson.* **2012**, *42*, 377 – 391.
[30] M. Gordon-Grossman, Y. Gofman, H. Zimmermann, V. Frydman, Y. Shai, N. Ben-Tal, D. Goldfarb, *J. Phys. Chem. B* **2009**, *113*, 12687 – 12695.
[31] M. Sammalkorpi, T. Lazaridis, *Biophys. J.* **2007**, *92*, 10 – 22.

